

FROM SOLAR AND STELLAR FLARES TO CORONAL HEATING: THEORY AND OBSERVATIONS OF HOW MAGNETIC RECONNECTION REGULATES CORONAL CONDITIONS

P. A. CASSAK,¹ D. J. MULLAN,¹ AND M. A. SHAY¹

Received 2007 October 16; accepted 2008 February 5; published 2008 March 3

ABSTRACT

There is currently no explanation of why the corona has the temperature and density it has. We present a model that explains how the dynamics of magnetic reconnection regulates the conditions in the corona. A bifurcation in magnetic reconnection at a critical state enforces an upper bound on the coronal temperature for a given density. We present observational evidence from 107 flares in 37 Sun-like stars that stellar coronae are near this critical state. The model may be important to self-organized criticality models of the solar corona.

Subject headings: stars: activity — stars: coronae — stars: flare — Sun: activity — Sun: corona — Sun: flares

1. INTRODUCTION

Dynamics in the solar corona takes on a wide range of forms. On one hand, the corona is the setting for the most violent eruptions in the solar system: solar flares and coronal mass ejections (Aschwanden et al. 2001). On the other, coronal heating makes the corona almost a thousand times hotter than the photosphere, even in the quiet Sun (Klimchuk 2006). Parker (1983, 1988) unified these two phenomena by proposing that micro- and nanoflares, less energetic cousins of eruptive flares, heat the corona. This model gained credence from studies showing that solar flares exhibit power-law statistics (Lin et al. 1984; Dennis 1985; Crosby et al. 1993; Feldman et al. 1997; Wheatland 2000; Nita et al. 2002; Paczuski et al. 2005) over a wide range of scales for many quantities. (See Charbonneau et al. [2001] for a review.) In addition, stellar flares have similar light curves to solar flares (Gershberg 2005) and also exhibit power-law statistics (Collura et al. 1988; Shakhovskaya 1989; Audard et al. 2000), suggesting that the physics of the solar corona is generic to Sun-like stars.

Coronal dynamics remains an active research area (Hudson 1991; Georgoulis et al. 1998; Shibata & Yokoyama 2002; Hughes et al. 2003). Details of the eruption process including how magnetic energy is stored, how eruptions onset, and how the stored energy is converted to other forms are still open questions. In addition, while micro- and nanoflares are believed to be a major contributor to coronal heating, the authors know of no theory that explains why the coronal temperature and density have the values they have, as opposed to larger or smaller values.

In this Letter, we propose that the condition of the corona is regulated by magnetic reconnection (Cassak 2006), a dynamical process that converts magnetic energy into kinetic energy and heat and energizes particles. Magnetic energy is stored during collisional (slow) reconnection, which has been shown to drive the coronal plasma toward lower collisionality (Cassak et al. 2006). If the plasma becomes marginally collisionless, a bifurcation in the underlying dynamics of reconnection occurs (Cassak et al. 2007b). This bifurcation, which occurs when two length scales δ_{SP} and ρ_i (to be defined below) are comparable, catastrophically initiates fast (Hall) reconnection, releasing the stored energy in the form of an eruption. The condition of marginal collisionality, therefore, sets an upper bound on how

hot the coronal plasma can be for a given density. The continual driving toward lower collisionality of the preflare corona by slow reconnection enforces the self-organization of the corona to a state of marginal collisionality where $\delta_{\text{SP}} \sim \rho_i$. We present finer details of this process below. Then, we perform the first observational test of this model using a large sample of data from stellar flares on Sun-like stars. We find that δ_{SP} and ρ_i are comparable for every event in the sample, indicating that stellar coronae do self-organize into a marginally collisional state.

2. THEORY

Magnetic reconnection depends strongly on the collisionality of the plasma. Collisional (Sweet-Parker) reconnection (Sweet 1958; Parker 1957) is exceedingly slow. The thickness δ_{SP} of the Sweet-Parker diffusion region is given by (Parker 1957)

$$\delta_{\text{SP}} \sim \sqrt{\frac{\eta c^2}{4\pi c_A}} L_{\text{SP}}, \quad (1)$$

where $c_A = B/(4\pi m_i n)^{1/2}$ is the Alfvén speed, B is the strength of the reconnecting magnetic field, m_i is the ion mass, n is the density, η is the resistivity, and L_{SP} is the length of the Sweet-Parker diffusion region in the outflow direction. The normalized reconnection rate $v_{\text{in}}/c_A \sim \delta_{\text{SP}}/L_{\text{SP}}$ is 10^{-7} for coronal parameters, where v_{in} is the inflow speed. Collisionless (Hall) reconnection has a reconnection rate of the order of 0.1 (Shay et al. 1999; Birn et al. 2001), 6 orders of magnitude faster than Sweet-Parker reconnection for coronal parameters.

Recent studies (Cassak et al. 2005, 2007a) showed that the transition from collisional to collisionless reconnection is catastrophic, occurring when δ_{SP} becomes smaller than the ion gyroradius ρ_i . At this scale, magnetohydrodynamics (MHD) breaks down and the Hall effect (absent in MHD) allows reconnection to be fast (Birn et al. 2001; Rogers et al. 2001). The transition can be described as a bifurcation (Cassak 2006; Cassak et al. 2007b) that takes stable equilibria out of existence as a control parameter ($\delta_{\text{SP}}/\rho_i$) varies. The relevant gyroradius ρ_i for antiparallel reconnection is the ion inertial scale d_i (Cassak et al. 2005),

$$d_i = \frac{c_A}{\Omega_{ci}} = \frac{c}{\omega_{pi}} = \sqrt{\frac{m_i c^2}{4\pi n e^2}}, \quad (2)$$

where Ω_{ci} is the ion cyclotron frequency, ω_{pi} is the ion plasma

¹ Department of Physics and Astronomy and Bartol Research Institute, University of Delaware, 217 Sharp Laboratory, Newark, DE 19716; pcassak@udel.edu, mullan@udel.edu, shay@physics.udel.edu.

frequency, and e is the ion charge. For reconnection with a (guide) magnetic field along the current sheet, the relevant gyroradius becomes $\rho_s = c_s/\Omega_{ci}$, where c_s is the sound speed (Cassak et al. 2007a).

To see how magnetic reconnection self-organizes the corona, consider an active region. Before an eruption, the plasma cannot be collisionless: if it were, the stored magnetic energy would be rapidly released by Hall reconnection. Therefore, the preflare active region must be collisional. Since (collisional) Sweet-Parker reconnection is exceedingly slow, magnetic energy can be stored. (By ‘‘collisional,’’ we mean $\delta_{sp} > d_i$, which, using eqs. [1] and [2], is equivalent to $\nu_{ie} > c_A/L_{sp}$, where $\nu_{ie} = \eta n e^2/m_i$ is the ion-electron collision frequency. Therefore, reconnection is collisional when the ion transit time along the Sweet-Parker diffusion region is longer than the ion-electron collision time. See also Uzdensky [2007b].)

When Sweet-Parker reconnection begins in the corona, e.g., as a result of two coronal flux tubes coming together, the reconnecting magnetic field B is initially much weaker than the strong asymptotic magnetic field in the core of the flux tube, i.e., the reconnection is embedded within a wider current sheet. From equation (1), a small B implies the thickness of the diffusion region will be relatively wide, so that $\delta_{sp} \gg \rho_i$. It was shown (Cassak et al. 2006) that embedded Sweet-Parker reconnection spontaneously self-drives the current sheet to thinner scales, even without external forcing. This is because the reconnection inflow convects stronger magnetic fields into the diffusion region, which causes δ_{sp} to decrease (see eq. [1]). Thus, the reconnection process itself self-drives the system toward lower collisionality.

If the asymptotic field is strong enough so that $\delta_{sp} \sim \rho_i$, i.e., the system becomes marginally collisionless, then a bifurcation causes Hall reconnection to begin, eruptively releasing the stored energy. (We note in passing that if B in an active region is not strong enough to ever satisfy $\delta_{sp} \sim d_i$ for a given density and temperature then no eruption occurs, potentially providing an observational constraint on which active regions erupt and which do not.) After the eruption, the corona returns to a collisional state, and the process begins again. The continual self-driving of the corona toward lower collisionality keeps coronal parameters near the critical condition where the bifurcation occurs ($\delta_{sp} \sim \rho_i$).

We propose that this process regulates the temperature of the corona. If the temperature T of the corona is larger than the critical value, the Spitzer resistivity η is smaller (since $\eta \propto T^{-3/2}$). From equation (1), a smaller η allows a smaller B to initiate an eruption. As such, less magnetic energy is stored and released, and the corona cools. Alternatively, if the corona is cooler than the critical value, a larger magnetic field is required to set off an eruption. More magnetic energy is stored and released, increasing the temperature. Either way, the temperature is driven back to the critical value. Uzdensky (2006, 2007a, 2007b) independently proposed a similar model based on the density, which we discuss in § 4.

3. OBSERVATIONAL DATA AND RESULTS

Observational verification of this model entails confirming that δ_{sp} and ρ_i are comparable at fast reconnection onset. Laboratory experiments (Ren et al. 2005; Egedal et al. 2007) are consistent with this condition, but direct observations of the corona are impossible because the length scales are not resolvable. Indirect verification is possible by estimating δ_{sp} and ρ_i for coronal parameters. For a solar active region, one finds

both length scales to be a few meters, as has been noted previously (Priest & Forbes 2000; Uzdensky 2003; Bhattacharjee 2004; Cassak et al. 2005, 2006; Uzdensky 2007b). An important question is whether this agreement is indicative of a general mechanism or is just a coincidence for solar parameters.

We use data from a recent study (Mullan et al. 2006) that analyzed 134 eruptive flares from 44 stars of spectral types F, G, K, and M, using the Deep Survey/Spectrometer Instrument on the *Extreme Ultraviolet Explorer (EUVE)* satellite. The data come from a single instrument on a single satellite, so there are no spurious variations due to different instrumental characteristics. See Mullan et al. (2006) for a thorough discussion of the data.

The e -folding time τ_d for the flare signal to decay and the emission measure EM were extracted from flare light curves. Because of interruptions in *EUVE* data during some flares, Mullan et al. (2006) presented the τ_d values for each flare as a unique value, a range of values, or an upper bound. We retain events having a particular value or a range (using the average) and omit events given as bounds, leaving 107 events from 37 stars.

Postflare parameters (the temperature T , density n , minimum magnetic field B_{min} , and length L and cross sectional area A of coronal loops) were derived (Mullan et al. 2006) from τ_d and EM using an approach due to Haisch (1983) that assumes that τ_d is comparable to the radiative and conductive cooling times. Taking $A \sim (L/10)^2$, one finds (Haisch 1983)

$$\begin{aligned} T(\text{K}) &= \alpha_T (\text{EM})^{0.25} \tau_d^{-0.25}, \\ n(\text{cm}^{-3}) &= \alpha_n (\text{EM})^{0.125} \tau_d^{-1.125}, \\ L(\text{cm}) &= \alpha_L (\text{EM})^{0.25} \tau_d^{0.75}, \end{aligned} \quad (3)$$

where $\alpha_T = 4 \times 10^{-5}$, $\alpha_n = 10^9$, and $\alpha_L = 5 \times 10^{-6}$ are constants (in cgs units). A lower bound for the magnetic field B_{min} is estimated by requiring the magnetic pressure $B^2/8\pi$ to be at least as large as the gas pressure $2nk_B T$, where k_B is Boltzmann’s constant, to maintain a coronal loop. As a test of the model, Mullan et al. (2006) surveyed the literature for independent measurements of T , n , L , and B_{min} for the stars in their study, finding that 178 of 212 measurements were consistent with the Haisch model. This justifies treating the derived parameters as valid independent of the Haisch model.

We first verify that the Haisch model gives reasonable results for solar parameters. Eruptive solar flares have $\tau_d \sim 10^4$ – 10^5 s and $\text{EM} \sim 10^{49}$ – 10^{50} cm^{-3} (Priest & Forbes 2000). Using these values, the Haisch model predicts postflare parameters of $T \sim 4$ – 13 MK, $n \sim (0.3$ – $5.6) \times 10^{10}$ cm^{-3} , $L \sim 10^{10}$ – 10^{11} cm, and $B_{min} \sim 10$ – 70 G. Compact solar flares have $\tau_d \sim 10^3$ s and $\text{EM} \sim 10^{47}$ – 10^{49} cm^{-3} (Priest & Forbes 2000). Using these values, the Haisch model gives $T \sim 4$ – 13 MK, $n \sim (3$ – $5) \times 10^{11}$ cm^{-3} , $L \sim (0.5$ – $1.6) \times 10^9$ cm, and $B_{min} \sim 90$ – 220 G. These ranges of T , n , L , and B_{min} are consistent with independent empirical values obtained from images and X-ray data for flaring loops in the Sun (Feldman et al. 1995; Shibata & Yokoyama 2002).

To calculate δ_{sp} and d_i from the Haisch model, we use B_{min} for the upstream magnetic field and n for the density. Sweet-Parker current sheets extend to system scales (Biskamp 1986), so L_{sp} is on the order of the coronal loop radius

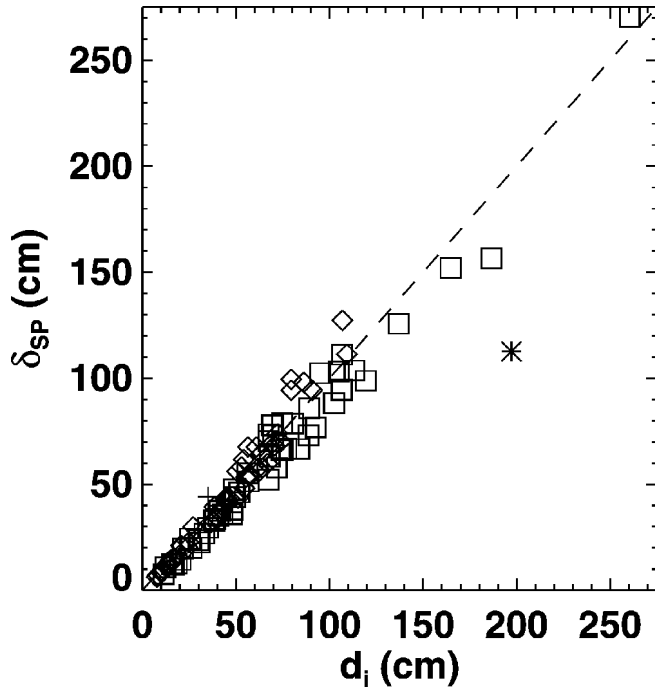


FIG. 1.—Sweet-Parker current layer thickness δ_{SP} vs. ion inertial length $d_i = c/\omega_{pi}$ for the stars in the sample. The dashed line displays their predicted equality. Boxes denote F, G, and K stars; diamonds denote M dwarfs. The asterisk at $d_i \sim 200$ cm and the plus sign at $d_i \sim 40$ cm denote values based on average τ_d and EM values for eruptive and compact solar flares, respectively (Priest & Forbes 2000).

$A^{1/2} \sim L/10$, consistent with the Haisch model. Finally, we use T to calculate the Spitzer resistivity (Spitzer & Härm 1953)

$$\eta = \frac{16\sqrt{\pi}e^2 \ln \Lambda}{3m_e} \left(\frac{m_e}{2k_B T} \right)^{3/2}, \quad (4)$$

where m_e is the electron mass and $\ln \Lambda = \ln [(3/2e^3)(k_B^3 T^3/\pi n)]^{1/2}$ is the Coulomb logarithm. Use of this formula is justified because the electron mean free path ($\lambda_{\text{mfpe}} \sim v_{\text{th,e}}/\nu_{ei} \sim 25$ km for solar conditions, where $v_{\text{th,e}}$ is the electron thermal speed and ν_{ei} is the electron-ion collision frequency) is small compared to length scales in the outflow direction ($L_{\text{SP}} \sim 10^4$ km) and along the current sheet ($L \sim 10^5$ km).

The result of comparing δ_{SP} to d_i using the stellar flare data is plotted in Figure 1. In addition, representative solar values based on $\tau_d = 10^{4.5}$ s and $\text{EM} = 10^{49.5} \text{ cm}^{-3}$ for eruptive flares ($\delta_{\text{SP}} \sim 110$ cm and $d_i \sim 200$ cm) and $\tau_d = 10^3$ s and $\text{EM} = 10^{48} \text{ cm}^{-3}$ for compact flares ($\delta_{\text{SP}} \sim 44$ cm and $d_i \sim 35$ cm) are plotted as the asterisk and plus sign, respectively. A dashed line with slope of unity is plotted. The agreement is extremely good. A least-squares analysis gives a best-fit slope of 0.98 ± 0.02 with a correlation coefficient of 0.981.

It is encouraging that the slope of the line in Figure 1 is consistent with unity. However, there are ambiguities in the data analysis. For example, we used d_i as the critical length scale, whereas ρ_s is more applicable to the corona (but more difficult to estimate). These scales differ by a factor of $\beta_{\text{tot}}^{1/2}$, where β_{tot} is the ratio of gas pressure to total magnetic pressure. If $\beta_{\text{tot}} \sim 0.1$ in the corona, this introduces a factor of a few. The present analysis does not intend to distinguish between the two gyroradii; rather, the results demonstrate that δ_{SP} is within

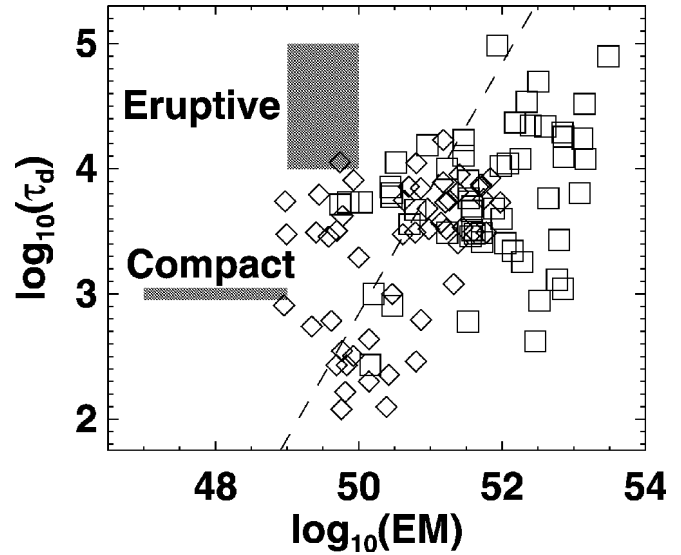


FIG. 2.—Decay time τ_d vs. emission measure EM for the stars in the sample. The dashed line shows the prediction of the theory. Boxes denote F, G, and K stars; diamonds denote M dwarfs. Ranges for eruptive and compact solar flares (Priest & Forbes 2000) are shown by the gray boxes.

a factor of a few of the critical length scale ρ_i in active stellar coronae.

A caveat of the result in Figure 1 pertains to how the parameters are derived in the Haisch model. Using equations (1), (2), and (4), using $L_{\text{SP}} \sim L/10$, and eliminating B by defining the ratio of gas pressure to magnetic pressure in the reconnecting magnetic field as $\beta_{\text{rec}} = 2nk_B T/(B^2/8\pi)$, we find $(\delta_{\text{SP}}/d_i)^2 \sim (e^4 \ln \Lambda/15k_B^2)(2\pi m_e \beta_{\text{rec}}/m_i)^{1/2}(nL/T^2)$. Treating β_{rec} as a fixed parameter and eliminating T , n , and L using equation (3) gives

$$\left(\frac{\delta_{\text{SP}}}{d_i} \right)^2 \sim \alpha \frac{\alpha_n \alpha_L}{\alpha_T^2} \ln \Lambda \sqrt{\beta_{\text{rec}}} \left(\frac{\tau_d}{\text{EM}} \right)^{1/8}, \quad (5)$$

where $\alpha = (e^4/15k_B^2)(2\pi m_e/m_i)^{1/2} = 1.09 \times 10^{-8} \text{ cm}^2 \text{ K}^2$ is a constant. The slow dependence on τ_d/EM significantly suppresses scatter in the observational data when evaluating δ_{SP}/d_i . However, the magnitude of δ_{SP}/d_i is unconstrained by the Haisch model, so the slope of the line in Figure 1 being of order unity is significant. Furthermore, since the data obtained using the Haisch model agree with independent determinations of the same quantities from other studies (Mullan et al. 2006), it is reasonable to assert that data obtained independently from the Haisch model would fall close to the same line.

We can avoid suppression of the scatter in the data by solving equation (5) for τ_d and taking a logarithm of both sides. This yields $\log(\tau_d) = \log(\text{EM}) + C$, where $C = 16 \log(\delta_{\text{SP}}/d_i) - 4 \log \beta_{\text{rec}} - 47$ using a value of $\ln \Lambda \sim 22$, which is representative of the stellar data in our study. If $\delta_{\text{SP}} \sim d_i$, this predicts a linear relationship between $\log(\tau_d)$ and $\log(\text{EM})$, with C being the y-intercept. The stellar data are plotted in Figure 2. The gray boxes show the range of values for eruptive and compact flares on the Sun (Priest & Forbes 2000). Assuming $\delta_{\text{SP}} \sim d_i$ and taking β_{rec} to be of order unity, the predicted line is plotted. While the data do not fall on a line, the line predicted by the hypothesis that $\delta_{\text{SP}} \sim d_i$ does pass through the data. To see why this is significant, note that if δ_{SP} was, say, $100d_i$ (at 1–10 m, still a very small length scale compared to coronal loop radii), then C would be -15 instead of -47 and the line in Figure 2 would lie 32 units higher, orders of magnitude

removed from the data. The hypothesis that $\delta_{\text{SP}} \sim d_i$ brings significant ordering to the data.

We note that the theory predicts $\delta_{\text{SP}} \sim d_i$ at flare onset, while the Haisch model refers to postflare conditions. Following an eruption on the Sun, temperatures typically increase by a factor of a few (Feldman et al. 1995), while the density increases due to chromospheric evaporation by at least a factor of 10 (compare preflare data [Schmelz et al. 1994] with postflare data [Doschek 1990]). From the relation above equation (5), $\delta_{\text{SP}}/d_i \propto n^{1/2}/T$. For an increase in n by a factor of 10 and T by a few, δ_{SP}/d_i does not change appreciably. Assuming this is true for other stars, if $\delta_{\text{SP}} \sim d_i$ after a flare, it is also true before a flare.

4. DISCUSSION

The data analyzed in this Letter pertain to flares in Sun-like stars, but the underlying dynamics of reconnection is general. Our model applies equally well to micro- and nanoflares in the quiet corona. Using values for the quiet Sun of $T \sim 1$ MK, $n \sim 10^9 \text{ cm}^{-3}$, $B \sim 5$ G, and $L \sim 10^{10}$ cm, we find $\delta_{\text{SP}} \sim 770$ cm and $d_i \sim 720$ cm, in agreement with the model.

The present result may have important implications for self-organized criticality (SOC) models of the solar corona. SOC occurs in driven, dissipative systems when the system is driven to a critical state where it undergoes a major reconfiguration (Bak et al. 1987). SOC leads to power-law statistics, which encouraged Lu & Hamilton (1991) to propose that the corona undergoes SOC. Subsequent studies of SOC in the corona exist (Lu et al. 1993; Vlahos et al. 1995; Longcope & Noonan 2000;

Islaker et al. 2001), but a firm physical foundation of the mechanism for self-driving and the physical condition setting the critical state is often traded for the ease of performing cellular automaton simulations (see Charbonneau et al. [2001] for a review). The present result provides a physical mechanism for self-driving (embedded Sweet-Parker reconnection) and the critical state (marginal collisionality), which may provide an avenue for developing quantitative predictions of SOC to compare with coronal observations.

An alternative mechanism (Uzdensky 2006, 2007a, 2007b) for heating the solar corona uses a change in density to achieve self-regulation. After an eruption, chromospheric evaporation increases the coronal density, decreasing the ion gyroradius (eq. [2]) and making subsequent eruptions more difficult. The extent to which Uzdensky's and our mechanisms regulate coronal heating is an open question.

The present model assumes that Sweet-Parker scaling is appropriate for thin current sheets of large extent. Long current sheets are known to fragment due to secondary instabilities, but the effect of this on the reconnection rate is unknown. Verification of the present model would entail testing whether Sweet-Parker reconnection in extended current sheets remains much slower than Hall reconnection. (See Uzdensky [2007b] for further discussion of this point as well as other future research directions.)

The authors thank J. F. Drake, A. Klimas, E. Ott, S. Owocki, P. So, and D. Uzdensky for helpful conversations. This work was supported in part by the Delaware Space Grant, NSF Grant ATM-0645271, and NASA Grant NNG05GM98G.

REFERENCES

- Aschwanden, M. J., Poland, A. I., & Rabin, D. M. 2001, *ARA&A*, 39, 175
 Audard, M., Gudel, M., Drake, J. J., & Kashyap, V. L. 2000, *ApJ*, 541, 396
 Bak, P., Tang, C., & Wiesenfeld, K. 1987, *Phys. Rev. Lett.*, 59, 381
 Bhattacharjee, A. 2004, *ARA&A*, 42, 365
 Birn, J., et al. 2001, *J. Geophys. Res.*, 106, 3715
 Biskamp, D. 1986, *Phys. Fluids*, 29, 1520
 Cassak, P. A. 2006, Ph.D. thesis, Univ. Maryland, <http://www.physics.udel.edu/~pcassak/cassakthesis.pdf>
 Cassak, P. A., Drake, J. F., & Shay, M. A. 2006, *ApJ*, 644, L145
 ———. 2007a, *Phys. Plasmas*, 14, 054502
 Cassak, P. A., Drake, J. F., Shay, M. A., & Eckhardt, B. 2007b, *Phys. Rev. Lett.*, 98, 215001
 Cassak, P. A., Shay, M. A., & Drake, J. F. 2005, *Phys. Rev. Lett.*, 95, 235002
 Charbonneau, P., McIntosh, S. W., Liu, H.-L., & Bogdan, T. J. 2001, *Sol. Phys.*, 203, 321
 Collura, A., Pasquini, L., & Schmitt, J. H. M. W. 1988, *A&A*, 205, 197
 Crosby, N. B., Aschwanden, M. J., & Dennis, B. R. 1993, *Sol. Phys.*, 143, 275
 Dennis, B. R. 1985, *Sol. Phys.*, 100, 465
 Doschek, G. A. 1990, *ApJS*, 73, 117
 Egedal, J., Fox, W., Katz, N., Porkolab, M., Reim, K., & Zhang, E. 2007, *Phys. Rev. Lett.*, 98, 015003
 Feldman, U., Doschek, G. A., & Klimchuk, J. A. 1997, *ApJ*, 474, 511
 Feldman, U., Laming, J. M., & Doschek, G. A. 1995, *ApJ*, 451, L79
 Georgoulis, M. K., Velli, M., & Einaudi, G. 1998, *ApJ*, 497, 957
 Gershberg, R. E. 2005, *Solar-Type Activity in Main-Sequence Stars* (Berlin: Springer)
 Haisch, B. M. 1983, in *IAU Colloq. 71, Activity in Red-Dwarf Stars*, ed. P. B. Byrne & M. Rodono (Dordrecht: Reidel), 255
 Hudson, H. S. 1991, *Sol. Phys.*, 133, 357
 Hughes, D., Paczuski, M., Dendy, R. O., Helander, P., & McClements, K. G. 2003, *Phys. Rev. Lett.*, 90, 131101
 Islaker, H., Anastasiadis, A., & Vlahos, L. 2001, *A&A*, 377, 1068
 Klimchuk, J. A. 2006, *Sol. Phys.*, 234, 41
 Lin, R. P., Schwartz, R. A., Kane, S. R., Pelling, R. M., & Hurley, K. C. 1984, *ApJ*, 283, 421
 Longcope, D. W. & Noonan, E. J. 2000, *ApJ*, 542, 1088
 Lu, E. T. & Hamilton, R. J. 1991, *ApJ*, 380, L89
 Lu, E. T., Hamilton, R. J., McTiernan, J. M., & Bromund, K. R. 1993, *ApJ*, 412, 841
 Mullan, D. J., Mathioudakis, M., Bloomfield, D. S., & Christian, D. J. 2006, *ApJS*, 164, 173
 Nita, G. M., Gary, D. E., Lanzerotti, L. J., & Thomson, D. J. 2002, *ApJ*, 570, 423
 Paczuski, M., Boettcher, S., & Baiesi, M. 2005, *Phys. Rev. Lett.*, 95, 181102
 Parker, E. N. 1957, *J. Geophys. Res.*, 62, 509
 ———. 1983, *ApJ*, 264, 642
 ———. 1988, *ApJ*, 330, 474
 Priest, E. & Forbes, T. 2000, *Magnetic Reconnection* (Cambridge: Cambridge Univ. Press)
 Ren, Y., Yamada, M., Gerhardt, S., Ji, H., Kulsrud, R., & Kuritsyn, A. 2005, *Phys. Rev. Lett.*, 95, 005003
 Rogers, B. N., Denton, R. E., Drake, J. F., & Shay, M. A. 2001, *Phys. Rev. Lett.*, 87, 195004
 Schmelz, J. T., Holman, G. D., Brosius, J. W., & Willson, R. F. 1994, *ApJ*, 434, 786
 Shakhovskaya, N. I. 1989, *Sol. Phys.*, 121, 375
 Shay, M. A., Drake, J. F., Rogers, B. N., & Denton, R. E. 1999, *Geophys. Res. Lett.*, 26, 2163
 Shibata, K. & Yokoyama, T. 2002, *ApJ*, 577, 422
 Spitzer, L. & Härm, R. 1953, *Phys. Rev.*, 89, 977
 Sweet, P. A. 1958, in *Electromagnetic Phenomena in Cosmical Physics*, ed. B. Lehnert (New York: Cambridge Univ. Press), 123
 Uzdensky, D. A. 2003, *ApJ*, 587, 450
 ———. 2006, preprint (arXiv:0607656)
 ———. 2007a, *Mem. Soc. Astron. Italiana*, 75, 282
 ———. 2007b, *ApJ*, 671, 2139
 Vlahos, L., Georgoulis, M., Kluiwing, R., & Paschos, P. 1995, *A&A*, 299, 897
 Wheatland, M. S. 2000, *ApJ*, 536, L109